SLAC-PUB-11381

An Ultra-High Gradient Cerenkov Wakefield Acceleration Experiment at SLAC FFTB

J.B.Rosenzweig[*], S. Hoover[*], M.J. Hogan[♣], P. Muggli[ℵ], M. Thompson[*], G. Travish[*], R. Yoder*

[*]*UCLA Dept. of Physics and Astronomy, 405 Hilgard Ave., Los Angeles, California 90095*
[♣]*Stanford Linear Accelerator Center, Stanford California 94309*
[ℵ]*University of Southern California, University Park Campus, Los Angeles, CA 90089*

Abstract: The creation of ultra-high current, ultra-short pulse beams (Q=3 nC, σ_z= 20 μm) at the SLAC FFTB has opened the way for very high gradient plasma wakefield acceleration experiments. We study here the use of these beams in a proposed Cerenkov wakefield experiment, where one may excite electromagnetic wakes in a simple dielectric tube with inner diameter of few100 microns that exceed the GV/m level. We discuss the scaling of the fields with design geometric design parameters, and choice of dielectric. We also examine measurable aspects of the experiment, such as the total coherent Cerenkov radiation energy one may collect, and the expected aspects of dielectric breakdown at high fields.

With the recent theoretical and experimental interest in laser acceleration, the issue of using dielectrics to support large accelerating fields has gained prominence. Various analyses have indicated that GV/m accelerating fields should be possible in dielectric-based laser accelerators[1], as long as illumination times are very short[2]. Dielectric accelerators may also be powered directly by charged particle beams, via wake-field excitation[3,4]. This mechanism has been studied in depth over the last several years, but with the maximum fields limited to 10's of MeV/m by the lack of ultra-short drive beams. According to scaling laws (described below), however, the recently achieved 20 μm pulse-length beams obtained at the SLAC FFTB SPPS facility may give over GV/m longitudinal fields. This possibility has led to a preliminary proposal, described in this paper, to use this beam in ultra-high field dielectric wakefield experiments.

Before discussing the experimental goals, we first present a heuristic analysis of the wakefields produced by the beam. In this analysis, as with the experiment, we refer to the schematic drawing of Fig. 1. To estimate the wakefields experienced by the beam, we note that the radial fields produced at the dielectric beam boundary at $r=a$ are

$$eE_r \cong -\frac{2N_b r_e m_e c^2}{\sqrt{2\pi}\sigma_z a}\exp\left(-\xi^2/2\sigma_z^2\right), \qquad (1)$$

where σ_z is the rms bunch length and $\xi = z - v_b t$. The radial field inside of the dielectric is smaller by ε^{-1}; additionally, we know that the angle of the field lines with respect to r is the Cerenkov angle[5], $\cos(\theta_c) = 1/\sqrt{\varepsilon}$, and the ratio of the longitudinal-to-transverse fields inside of the dielectric at $r=a$ is $E_z/E_r = \tan(\theta_c) = \sqrt{\varepsilon - 1}$. With continuity of E_z at the dielectric boundary, we have that the maximum decelerating electric field is

Contributed to 11th Advanced Accelerator Concepts Workshop (AAC 2004), June 21-26/2004, Stony Brook, New York
Work supported in part by Department of Energy contract DE-AC02-76SF00515

$$eE_{z\mathrm{dec}} \cong -\frac{2N_b r_e m_e c^2}{\sqrt{2\pi}\sigma_z a}\frac{\sqrt{\varepsilon-1}}{\varepsilon}\exp\left(-\xi^2/2\sigma_z^2\right). \tag{2}$$

We note that the decelerating field follows the beam current profile, a result that will be verified in simulation. This heuristic analysis is expected to give a good estimate as long as the radiated Cerenkov field does not reflect off of the conducting boundary at $r=b$, and superimpose field within the beam. Much more complete analyses based on traditional wakefield mode impedances are available in the literature[6,7,8,9], but these do not give numerical values for the field, or functional dependences on design parameters easily. We note that for the parameters given in Table 1, which are derived from known beam performance at the SPPS beam line, that the estimated decelerating field, which is nearly as large as the radial field at the dielectric boundary, is 4.25 GV/m. This is well above that expected to break down laser-excited structures. We will return to this point below.

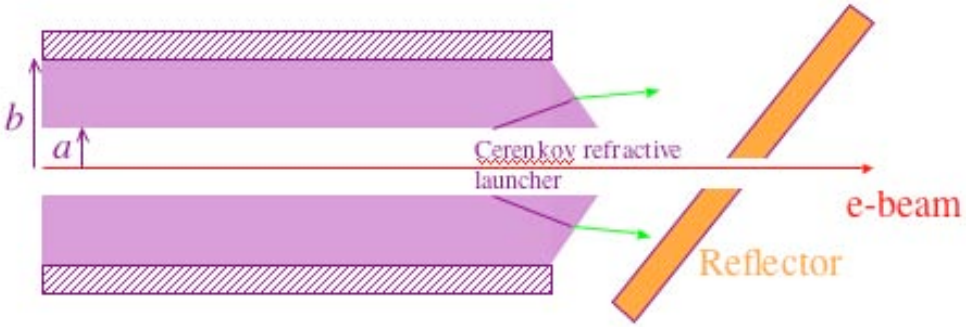

FIGURE 1. Geometry of Cerenkov wakefield experiment, using a metal-clad dielectric tube with inner radius *a* and outer radius *b*.

TABLE 1. Nominal parameters for Cerenkov wakefield experiment at SLAC FFTB.

Dielectric inner radius *a*	125 μm
Dielectric outer radius *b*	360 μm
Dielectric relative permittivity ε	3
Beam charge *Q*	3 nC
Rms bunch length σ_z	20 μm
Beam energy	30 GeV

In order to validate the model for energy loss to Cerenkov wakes, and explore implications of Eq. 2, we have performed a series of simulations using the code OOPIC[10]. An example of the output of such a simulation is shown in Fig. 2, which displays a map of the longitudinal field induced, from parameters slightly different from nominal, for aiding visualization. One can see that the decelerating field on the beam indeed is localized in a pulse that follows the beam current. The wakefield behind the beam propagates in the dielectric at the Cerenkov angle until it strikes the outer wall, and returns towards the axis. This wake waveform consists of many frequency components, which stay nearly coherent, reproducing a pulse structure repetitively behind the beam.

These frequency components can be deduced from the Cerenkov radiation propagation time in the dielectric, which for one "bounce" can be written as

$$T \cong \frac{2(b-a)\sqrt{\varepsilon}}{c\sin(\theta_c)} = \frac{2(b-a)}{c}\frac{\varepsilon}{\sqrt{\varepsilon-1}}. \tag{3}$$

The fundamental mode wavelength λ_1 excited in the structure, as well as its harmonics λ_n, can be approximated well using this time; the fundamental is the difference in the position of the Cerenkov front after two bounces, and the beam, which travels at nearly the speed of light,

$$\lambda_n \cong \frac{2cT}{n}\left(1-\frac{\cos(\theta_c)}{\sqrt{\varepsilon}}\right)=\frac{4(b-a)}{n}\frac{\varepsilon}{}\left(1-\frac{1}{\varepsilon}\right)=\frac{4(b-a)}{n}\sqrt{\varepsilon-1}\,. \tag{4}$$

This harmonic relationship can be seen in the wake waveform shown in Fig. 2, and examined quantitatively in the example plot of the on-axis value of E_z vs. *z* in Fig. 3. Here the prediction of Eq. 4 is for the distance between the positive E_z pulse and the negative pulse is, for Fig. 2, $\lambda_1/2$=2.82 mm, and for the parameters of Fig. 3, $\lambda_1/2$=0.68 mm. Both predictions are validated by the simulations.

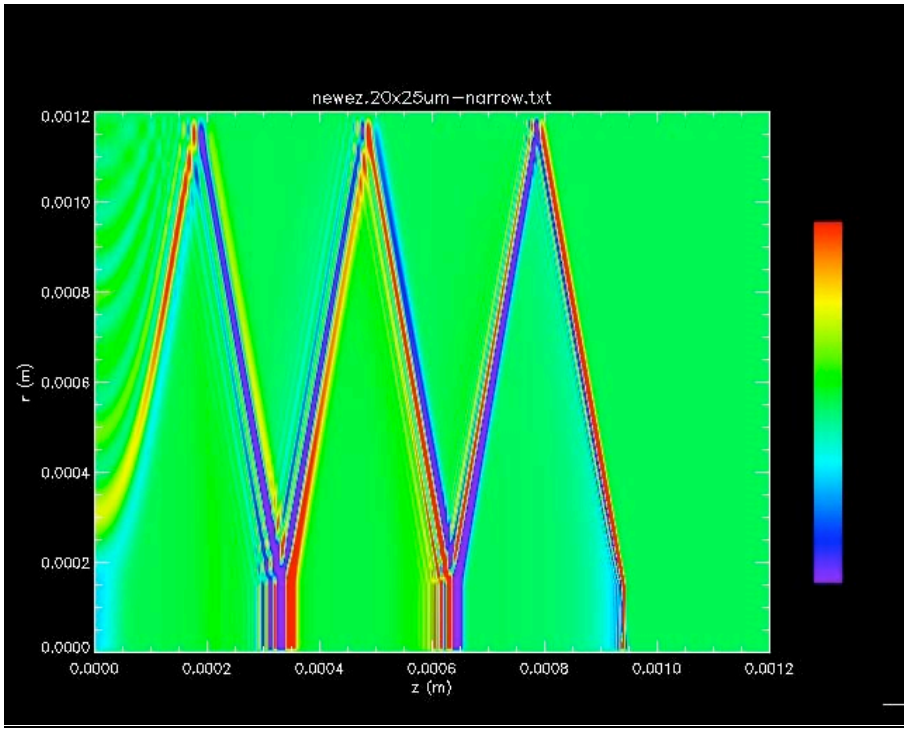

FIGURE 2. Example OOPIC simulation-derived false-color map of longitudinal electric field driven by a 2 nC, σ_z=20 μm, 30 GeV beam, propagating in a dielectric tube of 300 micron ID, 2.3 mm OD, and ε=3.

In order to evaluate the validity of the expression given in Eq. 2, as well as the acceleration fields behind the beam, we examine both the peak decelerating field inside of the beam, as well as the accelerating peak which trails, as shown in Fig. 3, which displays the on-axis value of E_z vs. *z*. The positive and negative peaks were deduced from such plots; the determination of the field inside of the beam suffers somewhat from noise.

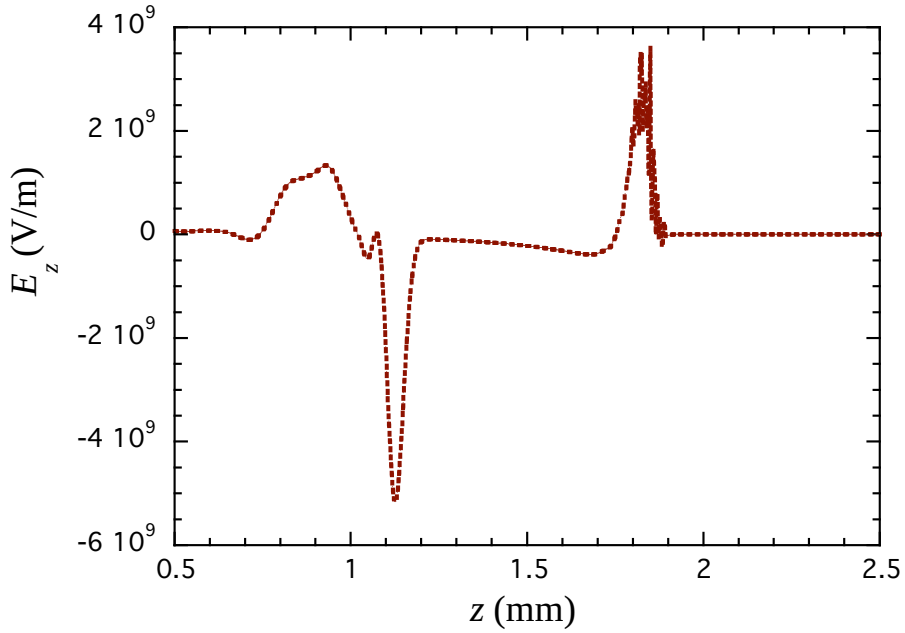

FIGURE 3. On-axis dependence of longitudinal field from OOPIC simulation- longitudinal electric field for case with Q=3 nC, σ_z=20 μm (centered at z=1.82 mm), 30 GeV beam, a=120 μm, b=360 μm, and ε=3.

Parametric studies of the fields' dependence on design parameters were performed with OOPIC, scanning over a range of a and b, and investigating the effect of ε choice. For the geometric scan, we kept constant the beam parameters: Q=3 nC, σ_z=20 μm, 30 GeV, and also took ε=3, while varying a and b, together, with b=3a. The results of this study are given in Fig. 4, in which we show the peak in the decelerating $E_{z,d,\max}$, the prediction of our heuristic theory for this quantity, and the first maximum in acceleration field, as a function of a. It can be seen the functional dependence of $E_{z,d,\max} \propto a^{-1}$ is well reproduced in simulations. The numerical prediction for $E_{z,d,\max}$ is quite close for our simple model, and is dominated by uncertainty in extracting this quantity from the simulation data in the presence of noise. We note that the rms beam size in the FFTB beam line at this point, $\sigma_x \cong 5$ μm, can be accommodated by this aperture. As noted in Table 1, the length of the tube is taken to be 1 cm, and so the transverse beam size is not a problem from the viewpoint of beam interception. It is, on the other hand, not reasonable to look at operation with the assumed beam and $a \leq 50$ μm, as the fields are already excessively high at this point.

For the scan of permittivity choice, we kept the beam parameters as before, and took a=120 μm, b/a=3. In Fig. 5, we plot the same quantities as in Fig. 4, but here as a function of ε. The heuristic model predicts that a maximum in decelerating field should be observed at ε=2, and this is reproduced by the simulations. The maximum is quite broad, however, and both quartz ($\varepsilon \cong 2.15$) and sapphire ($\varepsilon \cong 3$) would be good choices for maximizing the wakefield response.

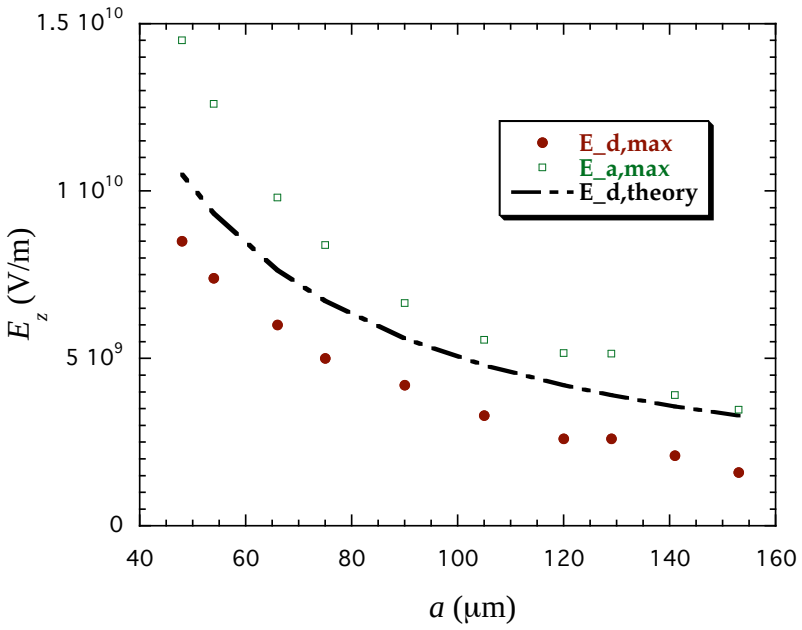

FIGURE 4. Dependence of longitudinal fields in Cerenkov wake simulations, with b/a=3, ε=3, and beam parameters Q=3 nC, σ_z=20 μm, energy of 30 GeV.

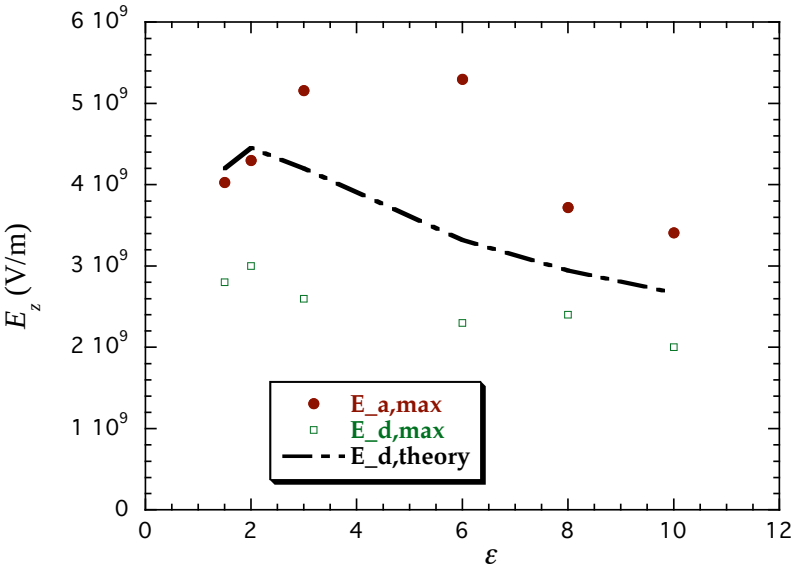

FIGURE 5. Dependence of longitudinal fields in Cerenkov wake simulations on ε, with a=120 μm, b/a=3, and beam parameters as in Figs. 3 and 4.

While one may calculate wakefield responses well in excess of GV/m, in practice this is the level at which we expect breakdown. Thus a series of experiments may be conceived of which explore breakdown, by changing either the beam parameters, or the dielectric tube geometry. At present, we are exploring the use of a "revolver" geometry, in which 6-8 tubes are loaded into a precision revolving mount. One of the tubes would be a metallic dummy, used only for alignment purposes. Note that as we are expecting energy loss rates at ~GeV/m, that the total energy change in the beam will be on the order

of 100 MeV, which is not measurable, given then that compression to 20 μm pulse length requires an energy spread of over 1 GeV.

In the proposed experiments, we therefore are interested in two signatures of high field Cerenkov wakes: detection of material breakdown and measurement of the coherent Cerenkov radiation produced. This proposed wakefield scenario is unique in that it may produce fields of interest in breakdown studies. We are particularly interested in learning the differences between material breakdown in wake-excited (very short pulse — sub-100 fs — relatively long wavelength) systems, as compared with optically (laser) excited systems. Quantum absorption of photons to produce free-electrons in the material is known to be an initiator of avalanche ionization. This mechanism may be mitigated in the wake experiment, thus allowing higher fields to be tolerated. For beam-derived fields in the beam geometry used here, the unipolar, large amplitude fields have led to extremely efficient ionization and plasma creation in the E164X plasma wakefield experiment. Possible detection methods for dielectric breakdown under present discussion include visible light from the discharge, and measuring current flow with a voltage bias imposed on the dielectric tube.

The propagating radiation fields associated with the energy loss of the beam also represent another robust experimental signal which can be exploited. The amount of energy lost to creating coherent Cerenkov radiation (CCR) power in our experimental scenario is approximated as

$$U_{\tilde{C}} \cong \frac{Q_b E_{z,\max}}{2} L_d \cong \frac{N_b^2 r_e m_e c^2}{\sqrt{2\pi}\sigma_z a} \frac{\sqrt{\varepsilon - 1}}{\varepsilon} L_d, \tag{5}$$

where L_d is the dielectric length. This radiation is emitted in narrow spectral lines, about wavelengths given approximately by Eq. 4. To estimate the energy in each wavelength, assuming that a large number of modes approximately equally spaced in frequency ω_n ($\Delta\omega = \pi c / 2(b-a)\sqrt{\varepsilon - 1}$, *cf.* Eq. 4) contribute to the flux, we note that Cerenkov radiation is inherently created with efficiency[11] proportional to ω_n, and also that the coherence[12] gives a multiplicative factor $N_b \exp\left(-\left(\omega_n \sigma_z / c\right)^2\right)$. Equating the integral of the over the mode contributions to the total of Eq. 5, we have

$$U_n \cong \left(\frac{\pi}{2}\right)^{3/2} \frac{n N_b^2 r_e m_e c^2 \sigma_z L_d}{2a(b-a)^2 \varepsilon \sqrt{\varepsilon - 1}} \exp\left[-\left(\frac{n\pi\sigma_z}{2(b-a)\sqrt{\varepsilon - 1}}\right)^2\right], \quad n = 1,2,3\ldots . \tag{6}$$

The energy in each line is approximately proportional to *n,* up until a roll-off wavelength at $\lambda_n \cong \sqrt{2\pi}\sigma_z$.

The overall amplitude of the coherent Cerenkov radiation (CCR) signal, for $N_b = 2 \times 10^{10}$, and $\sigma_z = 20$ microns, is 50 mJ, which is easily detectable by a variety methods, such as pyroelectric detectors and Golay cells. The collection of the radiation may be aided by using an appropriately shaped axicon-like geometry, as shown in Fig. 1, both to refract the radiation, and use Brewster angle incidence to suppress reflections at the boundary. As the overall geometry has two surfaces indicated that can induce transition radiation, coherent transition radiation (CTR) would be expected to form a significant background for this CCR measurement. The total CTR energy emitted can be estimated by looking at the total field energy in the beam outside of r_1. This radiation

(more correctly termed coherent diffraction radiation) energy can thus be estimated to have total energy

$$U_{CTR} \cong \iiint \frac{E_r^2}{4\pi} d^3x \cong \iiint \frac{N_b^2 \exp\left(-z^2/\sigma_z^2\right)}{2\pi^2 \sigma_z^2 r} dr d\phi dz \cong \frac{N_b^2 r_e m_e c^2}{\sqrt{\pi}\sigma_z} \ln\left(\frac{r_2}{r_1}\right). \tag{7}$$

The upper limit in the logarithm is a bit arbitrary (and unimportant), as it reflects the outer radius of the target. The ratio of the CCR to CCR energy, or signal-to-noise (STN), is thus

$$\frac{U_{\tilde{C}}}{U_{CTR}} \cong \frac{L_d}{a \ln(r_2/r_1)} \sqrt{\frac{\varepsilon - 1}{2\varepsilon^2}}. \tag{8}$$

For r_1=125 microns, r_2=2 cm, L_d=1 cm, and ε=3, we have a ratio of 5.2, which is an encouraging number. Note that because TR has a naturally flat spectrum, however, while CR grows as ω, STN should be quite improved for the highest frequencies, and high-pass filters should give further enhancement. Also, the CCR should have localized lines, as opposed to the broadband CTR spectrum, and so use of band-pass filters should allow a quite large improvement in STN.

Preliminary planning of an experiment at the FFTB using test-beam access is now underway. This test, which should be performed in the first half of 2005, will incorporate both experimental signatures for very large amplitude, coherent Cerenkov wake excitation discussed above.

ACKNOWLEGMENTS

This work is supported by U.S. Dept. of Energy grant DE-FG03-92ER40693.

REFERENCES

[1] J.B. Rosenzweig, A. Murokh, and C. Pellegrini, *Phys. Rev. Letters* **74**, 2467 (1995).
[2] D. Du, *et al., Appl. Phys. Lett.* **64**, 3073 (1994).
[3] W. Gai, *et al., Phys. Rev. Lett.* **61**, 2756 (1988).
[4] J.G. Power, et al., Phys. Rev. ST-Accel. Beams **3**, 101302 (2000)
[5] P. Cerenkov, *Dokl. Akad. Nauk* SSSR **2**, 451 (1934).
[6] King-Yuen Ng, *Phys. Rev. D* **42**, 1819 (1990).
[7] M. Rosing and W. Gai, *Phys. Rev. D* **42**, 1829 (1990).
[8] George Dome, in *Proceedings of the European Particle Accelerator Conference*, Nice, France 1990 (Editions Frontiers, Paris, 1990), p. 628.
[9] T-B. Zhang, J. L. Hirshfield, T. C. Marshall, and B. Hafizi, *Phys. Rev. E* **56**, 4647 (1997).
[10] D. L. Bruhwiler, *et al*. Phys. Rev. ST — Accel. Beams **4**, 101302 (2001).
[11] J.D. Jackson, *Classical Electrodynamics*, 2nd Ed, (Wiley, New York, 1975).
[12] Y. Shibata, *et al., Phys. Rev. E* **44**, R3449 (1991).